Molecular Microbiology (2004) **54**(5), 1287–1294 doi:10.1111/j.1365-2958.2004.04346.x

Inhibition of peptide bond formation by pleuromutilins: the structure of the 50S ribosomal subunit from *Deinococcus radiodurans* in complex with tiamulin

Frank Schlünzen,[1] Erez Pyetan,[2,3] Paola Fucini,[1] Ada Yonath[2,3] and Jörg M. Harms[2]*

[1]*Max-Planck Institute for Molecular Genetics, D-14195 Berlin, Germany.*

[2]*Max-Planck-Research-Unit for Ribosome Structure, D-22607 Hamburg, Germany.*

[3]*Weizmann Institute of Science, IL-76100 Rehovot, Israel.*

Summary

Tiamulin, a prominent member of the pleuromutilin class of antibiotics, is a potent inhibitor of protein synthesis in bacteria. Up to now the effect of pleuromutilins on the ribosome has not been determined on a molecular level. The 3.5 Å structure of the 50S ribosomal subunit from *Deinococcus radiodurans* in complex with tiamulin provides for the first time a detailed picture of its interactions with the 23S rRNA, thus explaining the molecular mechanism of the antimicrobial activity of the pleuromutilin class of antibiotics. Our results show that tiamulin is located within the peptidyl transferase center (PTC) of the 50S ribosomal subunit with its tricyclic mutilin core positioned in a tight pocket at the A-tRNA binding site. Also, the extension, which protrudes from its mutilin core, partially overlaps with the P-tRNA binding site. Thereby, tiamulin directly inhibits peptide bond formation. Comparison of the tiamulin binding site with other PTC targeting drugs, like chloramphenicol, clindamycin and streptogramins, may facilitate the design of modified or hybridized drugs that extend the applicability of this class of antibiotics.

Introduction

Tiamulin (Egger and Reinshagen, 1976a) is a derivative of the natural antibiotic pleuromutilin (Kavanagh *et al.*, 1951), which is a product of *Pleurotus mutilus* (nowadays called *Clitopilus scyphoides*). Tiamulin consists of a tricyclic nucleus composed of a cyclo-pentanone, cyclo-hexyl and cyclo-octane, and a (((2-(diethylamino)ethyl)thio)-acetic acid) side-chain on C14 of the octane ring (Fig. 1A). The drug is soluble in water and readily absorbed; it is therefore one of the few antibiotics that can be easily administered to animals. So far, pleuromutilin derivatives are only employed in veterinary practice and most frequently to treat swine dysentery. However, the increasing number of pathogens resistant to common antibiotics has raised a new interest in pleuromutilin derivatives, which may be suitable for human therapy (Brooks *et al.*, 2001; Bacque *et al.*, 2002; 2003; Pearson *et al.*, 2002; Springer *et al.*, 2003).

Early biochemical and genetic studies of the antimicrobial activity of tiamulin and other pleuromutilin derivates (Hodgin and Hogenauer, 1974; Drews *et al.*, 1975; Hogenauer, 1975; Egger and Reinshagen, 1976b) suggested that these antibiotics block peptide-bond formation directly by interfering with substrate binding at both the acceptor and donor sites of the ribosome's peptidyl-transferase center (PTC). On the other hand, it has been observed that ribosomes already engaged in the process of elongation are not influenced by these drugs (Dornhelm and Hogenauer, 1978).

Structural studies of complexes of ribosomal subunits with several clinically important antibiotics, e.g. macrolides, lincosamides, chloramphenicol or streptogramins, have significantly advanced the understanding of their inhibitory action (Brodersen *et al.*, 2000; Carter *et al.*, 2000; Pioletti *et al.*, 2001; Schlunzen *et al.*, 2001; Hansen *et al.*, 2002a; Berisio *et al.*, 2003a; 2003b; Hansen *et al.*, 2003; Schlunzen *et al.*, 2003; Harms *et al.*, 2004). However, the specific interactions of pleuromutilin drugs with the ribosome have so far escaped structural characterization.

To elucidate the antimicrobial activity of the pleuromutilins at the molecular level, we investigated the structure of the 50S ribosomal subunit from *Deinococcus radiodurans* (D50S) in complex with tiamulin. The 3.5 Å crystal structure allows the unambiguous localization of tiamulin in the 50S ribosomal subunits core region (Fig. 2), and provides a detailed picture of the specific interactions of tiamulin with 23S rRNA.

Accepted 11 August, 2004. *For correspondence. E-mail harms@riboworld.com; Tel. (+49) 40 89982809; Fax (+49) 40 89716810.

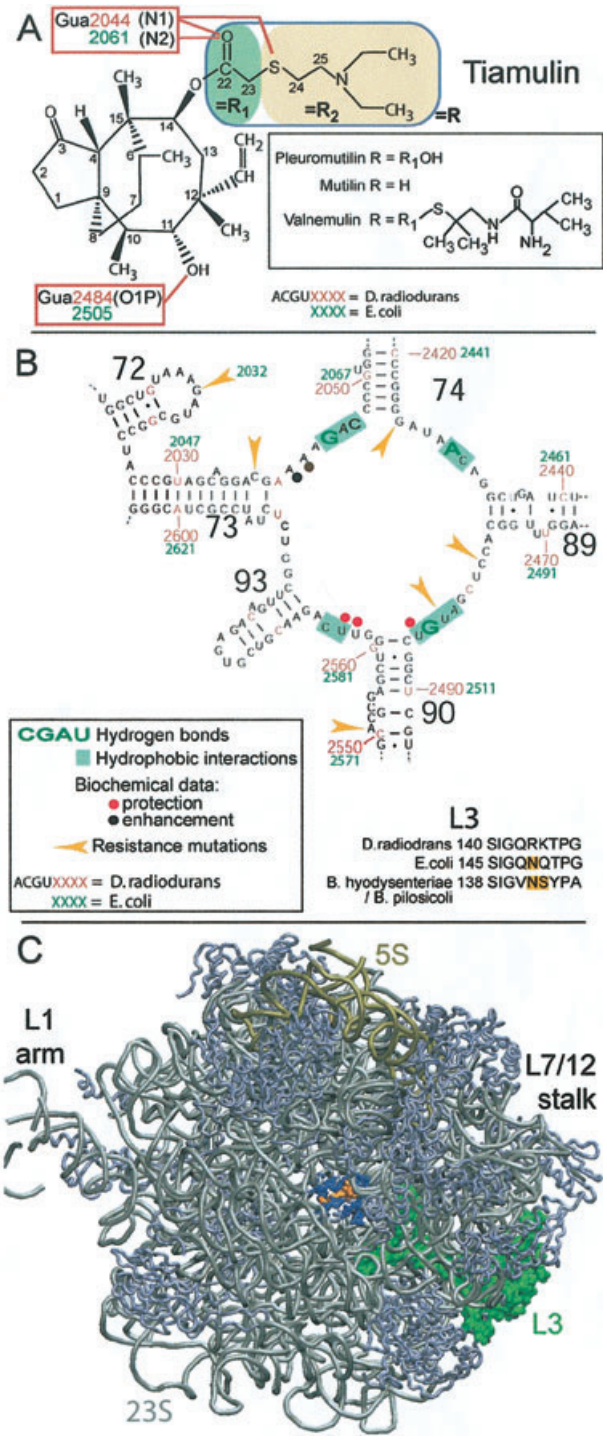

Fig. 1. Interactions of tiamulin with 23S rRNA.
A. 2D sketch of the chemical structure of tiamulin. The hydrogen bonds towards the 23S rRNA nucleotides are indicated, for *E. coli* (numbering in green) and for *D. radiodurans* (in red). The structural differences for pleuromutilin, mutilin and valnemulin are shown in a box for comparison.
B. Overview of the 23S rRNA nucleotides involved in tiamulin binding in comparison to those indicated by various biochemical and genetic experiments. The sequence itself corresponds to 23S rRNA of *D. radiodurans*. All other images use numbering according to *E. coli*.
C. A view down the ribosomal exit tunnel of the D50S ribosomal subunit. Tiamulin is marked in orange, its 23S rRNA binding partners in dark blue and ribosomal protein L3 is shown as a green surface model.

Results

Complexes of D50S with tiamulin were obtained by soaking native crystals in solutions containing tiamulin (see *Experimental procedures* for details). The crystals diffracted up to 3.3 Å, yielding sufficiently complete data to a resolution of 3.5 Å (see Table 1). The resulting electron density map was determining the drug's conformation and binding site within the large ribosomal subunit.

Tiamulin binds to the 23S rRNA through an extensive network of hydrophobic interactions involving exclusively nucleotides of domain V (namely G2061, A2062, C2063, A2451, C2452, A2503, U2504, G2505, U2506, U2585 and C2586) and through hydrogen bonds to G2061 and U2585 (Figs 1B and 2) (nucleotides are numbered according to the *Escherichia coli* 23S rRNA sequence throughout the text). The tricyclic nucleus of tiamulin is located inside a cavity confined by residues G2061, A2451, C2452, A2503, U2504, G2505, U2506 (Fig. 2B). It overlaps the position of A-site tRNA substrates, and is therefore expected to hamper A-site tRNA binding at the amino acid CCA-end (Fig. 3A and B). The cyclo-pentanone interacts with A2451 and C2452, whereas its keto group lies in close proximity to A2503 sugar. The cyclo-hexyl and its methyl at C6 interacts with A2451 and U2506 (Figs 1A and 2D). The cyclo-octane is not involved in significant interactions with 23S rRNA, whereas the methyls on positions C10, C12 and C15 and the ethyl group at C12 share hydrophobic interactions with G2061, C2063, A2451, A2503, U2504, G2505 and C2586. The only hydroxyl group of the molecule (on C11) offers a

Table 1. Crystal parameters and statistics of data collection and refinement.

Crystal information	
Space group	I222
Unit cell parameters (Å)	a = 168.7, b = 405.0, c = 693.0
Diffraction data statistics	
X-ray source/energy	ID29, ESRF, 13.7keV ID19, SBC/APS, 12.0keV
Crystal oscillation	0.1°
Resolution (Å)	30–3.5(3.56–3.5)
Completeness (%)	88.3 (76.7)
Rsym (%)	14.3 (34.1)
I/σ(I)	6.3 (1.8)
No. of reflections measured	1.658.726
No. of unique reflections	258.817
Refinement statistics	
R factor (%)	28.8
R free (%)	35.9
Bond distances rms (Å)	0.009
Bond angles rms	1.33°

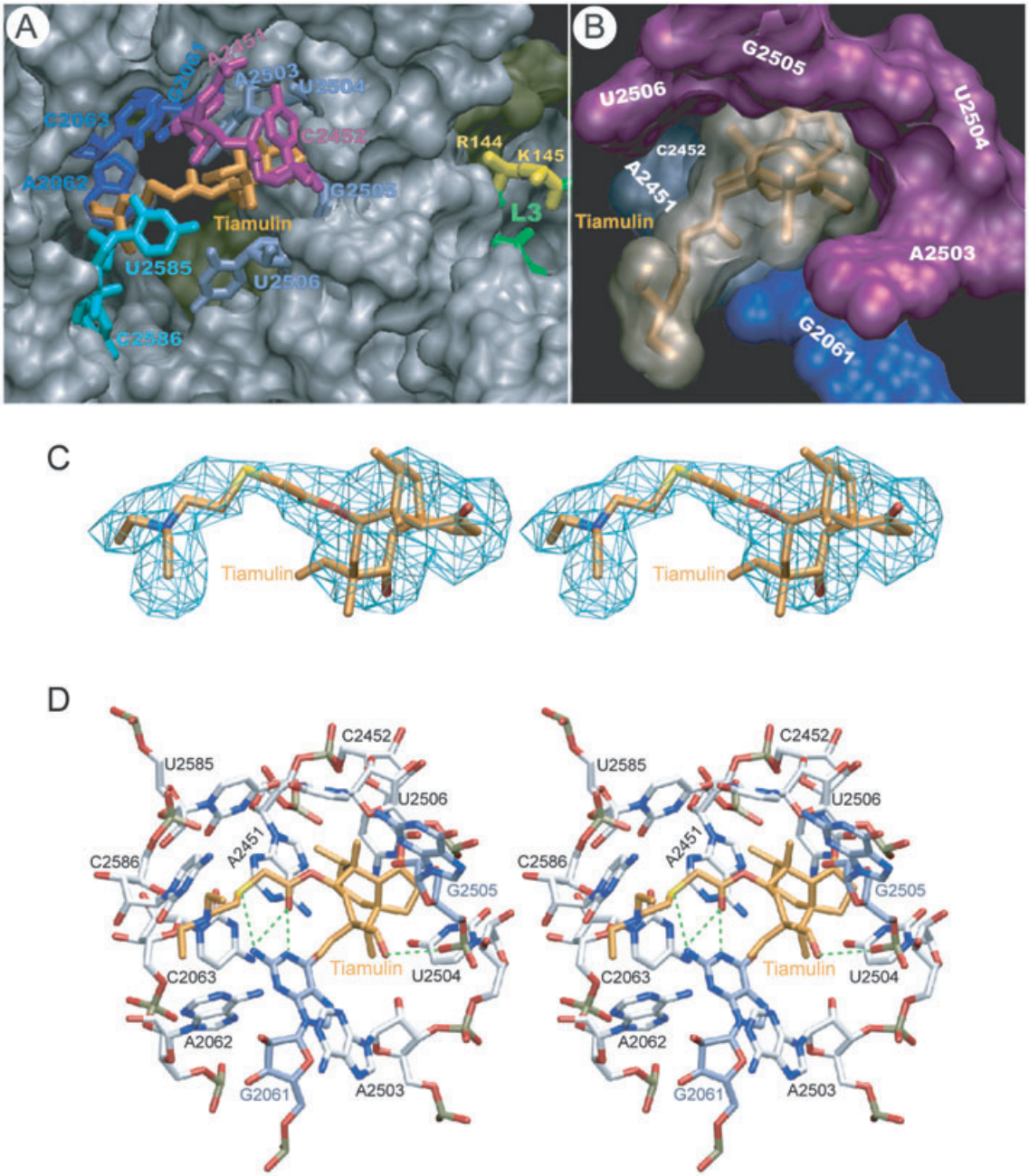

Fig. 2. Structure of tiamulin within the PTC.
A. Tiamulin (orange) is located in the PTC above the entrance to the ribosomal exit tunnel. 23S rRNA binding partners (various blues and purple), other rRNA nucleotides (grey) and ribosomal proteins (gold) are shown as surface representations. Ribosomal protein L3 is shown as green chain, whereas the two amino acids involved in resistance mutations are colored yellow.
B. The tricyclic nucleus of tiamulin (bones and transparent surface, orange) inside the rRNA cavity built of nucleotides G2061, A2451, C2452, A2503, U2504, G2505 and U2506 (colors as in A).
C. Stereo view of the electron density representing tiamulin. The compound has been omitted during calculation of the sigma weighted difference map; contouring is at 1.5σ.
D. Stereo view of the local environment of tiamulin (orange). Nucleotides involved in hydrogen bonds and hydrophobic interactions are colored in silver-blue and white respectively. Hydrogen bonds are shown as dotted green lines. For clarity nucleotides not involved in binding have been omitted.

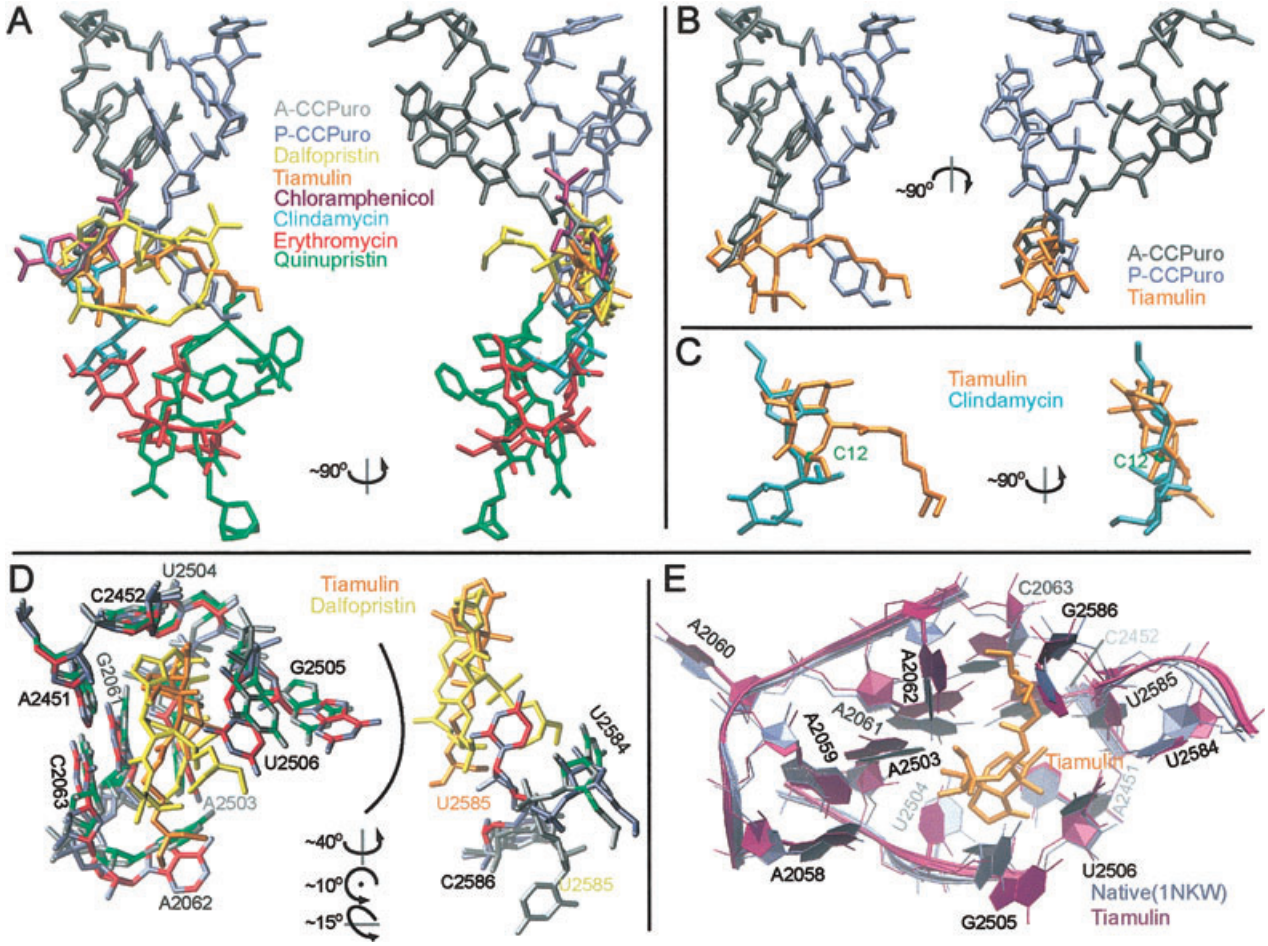

Fig. 3. Comparison of antibiotic binding sites within the PTC.
A. Structures have been aligned and overlaid to visualize the relative orientations of different classes of antibiotics and substrates in comparison to tiamulin: clindamycin (PDB entry 1JZX), erythromycin (1JZY), chloramphenicol (1K01), dalfopristin (1SM1), quinupristin (1SM1) and CC-Puromycin molecules as A- (A-CCPuro) and P-site (P-CCPuro) substrates. CC-Puromycin coordinates were taken from (Bashan *et al*., 2003) (1NJO). The right image shows a 90 degrees rotated orientation.
B. For a better visualization of the antibiotic action of tiamulin only the drugs A-CCPuro and P-CCPuro are shown in two orthogonal views.
C. Overlap of tiamulin with clindamycin. The left image shows a slightly rotated orientation relative to the view in (A); the right image is rotated by 90 degrees. The C12 position on the octane-ring of tiamulin is marked as a green ball.
D. Overlaid structures of dalfopristin and tiamulin. rRNA nucleotides obstructing the view have been omitted for clarity.
E. Comparison of native D50S (1NKW) and the tiamulin bound conformations.

hydrogen binding partner to O1P of G2505 and thus stabilizes the positioning of the tricyclic nucleus inside the cavity.

Based on tiamulin interactions with 23S rRNA, G2061 appears to be crucial for tiamulin binding: G2061 contributes to hydrophobic contacts with several side groups of the cyclo-octane of the nucleus. Moreover, it offers three hydrogen bonds altogether: between N1 or N2 of the purine and the keto on C22; and between N2 and the sulphur atom of the chain extruding from C14 of the mutilin core (Fig. 2D). This extension enhances the interactions of tiamulin with 23S rRNA through a hydrogen bond with C2063 contributed by the sulphur atom and a number of hydrophobic interactions with A2062, U2585 and C2586. Hence, it overlaps the position of P-site tRNA substrates (Fig. 3B).

Binding of tiamulin to the 50S subunit induces only a few local shifts in the 23S rRNA nucleotides (Fig. 3E), leaving the conformation of the individual bases largely unaffected. The most significant displacements are observed for G2505 (≈3 Å) and A2062 (≈2 Å), which transmit to their neighbouring nucleotides. These regions of 23S rRNA, 2503–2506 and 2061–2063, are precisely defining the binding pocket for the mutilin core of tiamulin. Modifications of these nucleotides or just suppression of the conformational changes induced by tiamulin must therefore severely reduce pleuromutilin susceptibility. The importance of 2061–2063 for the proper positioning and

stable binding of the pleuromutilin antibiotics in the PTC is further emphasized by the fact that mutilins lacking the C22-keto group do not exhibit antimicrobial activity (Egger and Reinshagen, 1976a).

Discussion

Tiamulin interacts with 23S rRNA

The crystallographic results presented here are well supported by previously published biochemical and genetic data. It has been shown that a number of rRNA bases: A2058, A2059, G2505, U2506 and U2585 within the PTC alter their reactivity to chemical probes in the presence of tiamulin or valnemulin (Poulsen *et al*., 2001). Most of these nucleotides were found to be directly involved in tiamulin binding (Fig. 1B). The reactivity of A2058–2059 is slightly enhanced in the presence of tiamulin and valnemulin, as is in the presence of dalfopristin, a streptogramin A antibiotic (Porse and Garrett, 1999). It is noteworthy that both compounds induce a similar shift of A2058 (Harms *et al*., 2004), which might explain the alteration of the reactivity of this base. A2058 is known to be essential for the binding of macrolides, streptogramins B and lincosamides (MLS_B) (Sigmund *et al*., 1984; Courvalin *et al*., 1985), and it seems that the small shift of A2058 induced by tiamulin binding should not disrupt contacts of the 23S RNA with macrolides like erythromycin. This agrees with the observation that tiamulin and erythromycin can bind concurrently (Poulsen *et al*., 2001).

The extension from the mutilin core is clearly responsible for the previously reported protection of U2506 and U2585 against DMS probing (Poulsen *et al*., 2001), as illustrated in (Fig. 1B). The authors further reported a similar but stronger protection of U2585 by valnemulin. This can be explained by the addition of two methyls at valnemulin's C23 (Fig. 1), which restricts the space available around U2585. Poulsen and coworkers have also observed that U2584 is less accessible to CMTC in the presence of both drugs. The present structure shows no involvement of U2584 in tiamulin binding, suggesting that its effect must be indirect. However, the binding of tiamulin to U2506, U2585 and G2586 rigidifies the local conformation and reduces the space between U2584 and the tunnel (Fig. 3E) which can account for the change in accessibility.

Pringle and coworkers (Pringle *et al*., 2004) characterized tiamulin resistant mutants in *Brachyspira* spp. isolates. Interestingly, all the mutations cluster around U2504, and because nucleotides 2503–2506 are actively involved in tiamulin binding, these results are in good agreement with the structural data. Nucleotides 2503–2505 partially define the binding pocket for the mutilin core of tiamulin. Any alterations within this region, particularly those reducing the solvent accessible surface, would inhibit binding of pleuromutilin antibiotics.

Remote effect of ribosomal protein L3

The mutilin core binding pocket is also targeted by remote modifications that are transmitted over a distance of 10–12 Å: a number of tiamulin resistant strains that contain mutations in ribosomal proteins L3 at *E. coli* positions 148 or 149 have been found (Bosling *et al*., 2003; Pringle *et al*., 2004). In *D. radiodurans* the corresponding amino acids (144 145) are located on the loop-like extension of L3 reaching towards the PTC (Figs 1C and 2A) (Harms *et al*., 2001). This region of L3 exhibits a particularly high sequence variability among different bacterial species. It implies that the loop of L3 is not dictating a specific 23S rRNA structure, but rather restraints its conformational freedom. Hence, these mutations of L3 are presumed to alter the flexibility of this region, which by itself is usually not sufficient to obtain a high degree of resistance against tiamulin (Pringle *et al*., 2004). All L3 mutations that could be correlated with strong resistance against tiamulin were accompanied by additional 23S rRNA mutation (Pringle *et al*., 2004). Only the combined effect of L3 and 23S rRNA mutations aptly restricts the local conformation to render the binding pocket inaccessible for tiamulin, thus yielding a highly resistant species.

Antibiotic specificity

Tiamulin clearly interferes with the correct positioning of both A- and P-site substrates (Fig. 3B). Like the streptogramin A compound dalfopristin (Harms *et al*., 2004), tiamulin effectively blocks the universally conserved nucleotide U2585 (Fig. 3D), which is an essential element for the elongation of the nascent peptide and the translocation of the tRNAs (Nissen *et al*., 2000; Hansen *et al*., 2002b; Schmeing *et al*., 2002; Bashan *et al*., 2003). Hence, tiamulin might affect the formation of the 70S initiation complex by interfering with proper positioning of the initiator tRNA in the P-site (Fig. 3B). Based on the chemical structures of the different pleuromutilin compounds, it is expected that this effect is more pronounced for tiamulin and valnemulin than for pleuromutilin, which lacks the long C14-extension. Even if the CCA-3′-end of the P-site tRNA might be sufficiently flexible to allow binding in the presence of tiamulin, the correct positioning of the peptides attached to the tRNAs will be strongly affected. Peptide bond formation as well as the puromycin fragment reaction should therefore be inhibited by tiamulin, in agreement with biochemical data (Hogenauer, 1975; Poulsen *et al*., 2001). On the other hand, tiamulin will not bind to the 50S subunit, while the A- or the P-site is occupied. This supports previously published results

showing that ribosomes engaged in elongation are not susceptible to tiamulin (Dornhelm and Hogenauer, 1978).

Binding of tiamulin in comparison with other 50S inhibitors

Tiamulin is known to compete for binding to the 50S ribosomal subunit with chloramphenicol, puromycin (Hogenauer *et al*., 1981) and carbomycin A (Poulsen *et al*., 2001). Our structure shows that the binding site of tiamulin overlaps those of chloramphenicol and clindamycin (Schlunzen *et al*., 2001) (Fig. 3A and C) as well as that of the di-sacharine branch of carbomycin A (Hansen *et al*., 2002a).

Tiamulin binds in almost the same position as dalfopristin (Harms *et al*., 2004) or virginiamycin A (Hansen *et al*., 2003), both belonging to the streptogramin A class of antibiotics. This is somewhat surprising because tiamulin and dalfopristin do not share any structural similarity, except for the (2-(diethylamino)ethyl)-extension, which differs, however, in terms of position, interactions or environment (Fig. 3D).

Comparison between the conformation of the 23S rRNA nucleotides within the tiamulin- and dalfopristin-complex reveals only two significant differences. One concerns U2585, which is rotated by almost 180 degrees in the streptogramin complex compared to the orientation in the native structure or the tiamulin-D50S complex (Harms *et al*., 2004). The other deviation is observed for A2062, which obtains a specific orientation facilitating simultaneous binding of streptogramin A and B compounds (Fig. 3D).

The similarity between the binding positions of tiamulin and dalfopristin and the largely identical local conformation of 23S rRNA suggest that tiamulin could also lead to a synergistic enhancement of streptogramin B binding. Preliminary structural analysis of D50S crystals soaked in solutions containing both tiamulin and mikamycin B revealed, however, that mikamycin B does not bind in the presence of tiamulin, and tiamulin binding remains unaffected (E. Pyetan, F. Schlünzen, and J. Harms, unpubl. data). This confirms the low affinity of streptogramins B in the absence of their synergistic counterpart (Parfait and Cocito, 1980), and rules out an enhancement of streptogramin B binding by tiamulin. Presumably, the conformation of A2062 induced by streptogramins A but not by tiamulin seems to be indispensable for streptogramin B binding.

Nevertheless, the structure of the tiamulin-50S complex suggests modifications, which could result in the enhancement of antimicrobial activity. For example, it might be possible to combine clindamycin and pleuromutilins in such a way that the sugar-moiety of clindamycin would serve as a potential C12-extension of the pleuromutilins cyclo-octane. On the other hand, the methyl group of the (((2-(diethylamino)ethyl)thio)-acetic acid) side-chain of tiamulin is within binding distance to the ethyl group on the macrocyclic ring of quinupristin (Fig. 3A). Although attachment of the thio-acetic moiety to streptogramins B would prevent synergistic binding, it might still substantially enhance streptogramin B binding. Such a modified streptogramin would not only block the entrance to the ribosomal exit tunnel, but also affect peptide bond formation directly.

Conclusion

Tiamulin was found to bind tightly in a cavity within the PTC of the 50S ribosomal subunit. The binding site of tiamulin overlaps that of both A- and P-site tRNA substrates and thus explains its direct inhibition of peptide bond formation. The results are in agreement with almost all biochemical and genetic data previously published (Fig. 1B). Particularly, most of the mutations that reduce tiamulin susceptibility affect the conformation or flexibility of the 23S rRNA nucleotides, which delineate the mutilin binding pocket. Cross-resistances and competitions with other 50S inhibitors result from the overlap of Tiamulin's position with the binding sites of antibiotics like dalfopristin (streptogramin A), chloramphenicol and clindamycin (Fig. 3A, C and D). The partial overlap of different antibiotics might hint towards hybridization or modification of the known compounds and this may suggest the design of compounds with an enhanced antimicrobial activity.

Experimental procedures

Base and amino acid numbering

Nucleotides named [ACGU]1234 are numbered according to the sequence of 23S RNA from *E. coli* to permit a direct comparison with biochemical data. A conversion of base numbers between *E. coli* and *D. radiodurans* for the binding region of tiamulin can be found in Fig. 1B. Translation tables converting the full 23S rRNA sequence of *D. radiodurans* to *E. coli* and to *Haloarcula marismortui* are available from the authors or at http://www.riboworld.com/nuctrans/. 23S rRNA sequence alignments were based on the 2D-structure diagrams obtained from Cannone *et al*. (2002).

Crystallization

Crystals of 50S belong to the space group I222 and contain one particle per asymmetric unit. Crystals were grown within 2–4 weeks by vapor diffusion, in 10 mM $MgCl_2$, 60 mM NH_4Cl, 5 mM KCl, 10 mM HEPES, pH 7.8, using low concentrations (0.1–1%) of poly and monovalent alcohols (dimethylhexandiol:ethanol) as precipitant (Harms *et al*., 2001). Because the long-term stability of tiamulin at pH > 7 is relatively poor, tiamulin complexes could not be obtained by cocrystallization. The preformed D50S crystals were therefore soaked for 12 h in their harvesting solution containing 0.01 mM tiamulin. Crystals were then briefly transferred to a

cryo-buffer containing 13–15% of dimethyl-hexandiol and ethanol prior to freezing the crystals in liquid propane.

X-ray diffraction

Initial diffraction quality tests were performed at BW6, HASYLAB/DESY. Data were collected at 85 K from shock-frozen crystals with synchrotron radiation beam at ID19, Argonne Photon Source/Argonne National Laboratory and ID29, European Synchrotron Radiation Facility/European Molecular Biology Laboratory. Data were recorded on MAR CCD, ADSC-Quantum 4 or APS-CCD detectors and processed with HKL2000 (Otwinowski and Minor, 1997) and the CCP4 suite (Bailey, 1994). See Table 1 for data statistics.

Localization and refinement

The native structure of D50S was refined against the structure factor amplitudes of the antibiotic complex using rigid body refinement as implemented in CNS (Brunger *et al*., 1998). For free R-factor calculation, 5% of the data were omitted during refinement. The antibiotic site was readily determined from sigmaA weighted difference maps. To obtain an unbiased electron density map, tiamulin as well as its local 23S rRNA environment has been omitted from these calculations. To enhance the details, the difference maps were subjected to density modification using the CCP4 package suite (Bailey, 1994). The quality of the difference maps unambiguously revealed the position and orientation of tiamulin. Finally, restraint minimization was carried out using CNS (Brunger *et al*., 1998). See Table 1 for refinement statistics.

Coordinates and figures

As there is currently no 3D-structure for tiamulin (6-ethenyl-decahydro-5-hydroxy-4,6,9,10-tetramethyl-1-oxo-3a,9-propano-3aH-cyclopentacycloocten-8-yl ester (3aS-(3aalpha, 4beta, 5alpha, 6alpha, 8beta, 9alpha, 9abeta, 10S*))), we used the tricyclic nucleus of O-bromoacetyl-pleuromutilin (CSD-entry BAPLEU) combined with the C14-side-chain from a tiamulin structure generated with the program CORINA (http://www2.chemie.uni-erlangen.de/software/corina/index.html) for map fitting. The C14-side-chain was further refined according to the electron density, and finally the complete molecule was subjected to energy minimization with CNS.

3D-figures were produced with VMD (Humphrey *et al*., 1996). The ribosome–antibiotic interactions were originally determined with LigPlot (Wallace *et al*., 1995), but were represented in a sketched manner for clarity (Figs 1 and 3D). Final coordinates have been deposited in the Protein Data Bank under accession number 1XBP.

Acknowledgements

We gratefully acknowledge Märit Pringle, Birte Vester and colleagues for sharing their data on tiamulin resistance prior to publication. We thank the members of the ribosome groups in Hamburg (MPG-ASMB), in Berlin (MPI for Molecular Genetics) and Rehovot (Weizmann Institute) for their invaluable contributions. Special thanks go to M. Dobler and M. Swairjo for help on the tiamulin molecule structure, and Birte Vester for her critical comments on the manuscript. These studies could not be performed without the excellent support by the staff of the MPG beamline BW6 at HASYLAB/DESY, the ESRF beamlines ID14-2/4 and ID29 and the APS/SBC beamline ID-19. Use of the Argonne National Laboratory Structural Biology Center beamline at the Advanced Photon Source was supported by the U. S. Department of Energy, Office of Biological and Environmental Research, under Contract No. W-31–109-ENG-38. We acknowledge the European Synchrotron Radiation Facility for provision of synchrotron radiation facilities. Support was provided by the Max-Planck-Society, the US National Institutes of Health (GM34360), the German Ministry for Science and Education (BMBF Grant 05–641EA) and the Kimmelman Center for Macromolecular Assembly at the Weizmann Institute. A.Y. holds the Martin S. and Helen Kimmel Professorial Chair.

References

Bacque, E., Pautrat, F., and Zard, S.Z. (2002) A flexible strategy for the divergent modification of pleuromutilin. *Chem Commun (Camb)* **20:** 2312–2313.

Bacque, E., Pautrat, F., and Zard, S.Z. (2003) A concise synthesis of the tricyclic skeleton of pleuromutilin and a new approach to cycloheptenes. *Org Lett* **5:** 325–328.

Bailey, S. (1994) The Ccp4 Suite – Programs for Protein Crystallography. *Acta Crystallogr D Biol Crystallogr* **50:** 760–763.

Bashan, A., Agmon, I., Zarivach, R., Schluenzen, F., Harms, J., Berisio, R., *et al.* (2003) Structural basis of the ribosomal machinery for peptide bond formation, translocation, and nascent chain progression. *Mol Cell* **11:** 91–102.

Berisio, R., Harms, J., Schluenzen, F., Zarivach, R., Hansen, H.A., Fucini, P., and Yonath, A. (2003a) Structural Insight into the Antibiotic Action of Telithromycin against Resistant Mutants. *J Bacteriol* **185:** 4276–4279.

Berisio, R., Schluenzen, F., Harms, J., Bashan, A., Auerbach, T., Baram, D., and Yonath, A. (2003b) Structural insight into the role of the ribosomal tunnel in cellular regulation. *Nat Struct Biol* **10:** 366–370.

Bosling, J., Poulsen, S.M., Vester, B., and Long, K.S. (2003) Resistance to the peptidyl transferase inhibitor tiamulin caused by mutation of ribosomal protein l3. *Antimicrob Agents Chemother* **47:** 2892–2896.

Brodersen, D.E., Clemons, W.M., Jr, Carter, A.P., Morgan-Warren, R.J., Wimberly, B.T., and Ramakrishnan, V. (2000) The structural basis for the action of the antibiotics tetracycline, pactamycin, and hygromycin B on the 30S ribosomal subunit. *Cell* **103:** 1143–1154.

Brooks, G., Burgess, W., Colthurst, D., Hinks, J.D., Hunt, E., Pearson, M.J., *et al.* (2001) Pleuromutilins. Part 1. The identification of novel mutilin 14-carbamates. *Bioorg Med Chem* **9:** 1221–1231.

Brunger, A.T., Adams, P.D., Clore, G.M., DeLano, W.L., Gros, P., Grosse-Kunstleve, R.W., *et al.* (1998) Crystallography & NMR system: a new software suite for macromolecular structure determination. *Acta Crystallogr D Biol Crystallogr* **54:** 905–921.

Cannone, J.J., Subramanian, S., Schnare, M.N., Collett, J.R., D'Souza, L.M., Du, Y., *et al.* (2002) The Comparative RNA Web (CRW) Site: an online database of comparative sequence and structure information for ribosomal, intron, and other RNAs: Correction. *BMC Bioinformatics* **3:** 15.

Carter, A.P., Clemons, W.M., Brodersen, D.E., Morgan-Warren, R.J., Wimberly, B.T., and Ramakrishnan, V. (2000) Functional insights from the structure of the 30S ribosomal subunit and its interactions with antibiotics. *Nature* **407:** 340–348.

Courvalin, P., Ounissi, H., and Arthur, M. (1985) Multiplicity of macrolide-lincosamide-streptogramin antibiotic resistance determinants. *J Antimicrob Chemother* **16 (**Suppl. A): 91–100.

Dornhelm, P., and Hogenauer, G. (1978) The effects of tiamulin, a semisynthetic pleuromutilin derivative, on bacterial polypeptide chain initiation. *Eur J Biochem* **91:** 465–473.

Drews, J., Georgopoulos, A., Laber, G., Schutze, E., and Unger, J. (1975) Antimicrobial activities of 81.723 hfu, a new pleuromutilin derivative. *Antimicrob Agents Chemother* **7:** 507–516.

Egger, H., and Reinshagen, H. (1976a) New pleuromutilin derivatives with enhanced antimicrobial activity. II. Structure-activity correlations. *J Antibiot (Tokyo)* **29:** 923–927.

Egger, H., and Reinshagen, H. (1976b) New pleuromutilin derivatives with enhanced antimicrobial activity. I. Synthesis. *J Antibiot (Tokyo)* **29:** 915–922.

Hansen, J.L., Ippolito, J.A., Ban, N., Nissen, P., Moore, P.B., and Steitz, T.A. (2002a) The structures of four macrolide antibiotics bound to the large ribosomal subunit. *Mol Cell* **10:** 117–128.

Hansen, J.L., Schmeing, T.M., Moore, P.B., and Steitz, T.A. (2002b) Structural insights into peptide bond formation. *Proc Natl Acad Sci USA* **99:** 11670–11675.

Hansen, J.L., Moore, P.B., and Steitz, T.A. (2003) Structures of five antibiotics bound at the peptidyl transferase center of the large ribosomal subunit. *J Mol Biol* **330:** 1061–1075.

Harms, J., Schluenzen, F., Zarivach, R., Bashan, A., Gat, S., Agmon, I., *et al.* (2001) High resolution structure of the large ribosomal subunit from a mesophilic eubacterium. *Cell* **107:** 679–688.

Harms, J.M., Schluenzen, F., Fucini, P., Bartels, H., and Yonath, A.E. (2004) Alterations at the peptidyl transferase centre of the ribosome induced by the synergistic action of the streptogramins dalfopristin and quinupristin. *BMC Biology* **2:** 1–10.

Hodgin, L.A., and Hogenauer, G. (1974) The mode of action of pleuromutilin derivatives. Effect on cell-free polypeptide synthesis. *Eur J Biochem* **47:** 527–533.

Hogenauer, G. (1975) The mode of action of pleuromutilin derivatives. Location and properties of the pleuromutilin binding site on Escherichia coli ribosomes. *Eur J Biochem* **52:** 93–98.

Hogenauer, G., Egger, H., Ruf, C., and Stumper, B. (1981) Affinity labeling of Escherichia coli ribosomes with a covalently binding derivative of the antibiotic pleuromutilin. *Biochemistry* **20:** 546–552.

Humphrey, W., Dalke, A., and Schulten, K. (1996) VMD: visual molecular dynamics. *J Mol Graph Model* **14:** 27–38.

Kavanagh, F., Hervey, H., and Robbins, W.J. (1951) Antibiotic Substances from Basidiomycetes. VIII. Pleurotus multilus (fr.) Sacc. & Pleurotus Passeckerianus Pilat. *Proc Natl Acad Sci USA* **37:** 570–574.

Nissen, P., Hansen, J., Ban, N., Moore, P.B., and Steitz, T.A. (2000) The structural basis of ribosome activity in peptide bond synthesis. *Science* **289:** 920–930.

Otwinowski, Z., and Minor, W. (1997) Processing of X-ray diffraction data collected in oscillation mode. *Macromolecular Crystallogr* **276:** 307–326.

Parfait, R., and Cocito, C. (1980) Lasting damage to bacterial ribosomes by reversibly bound virginiamycin M. *Proc Natl Acad Sci USA* **77:** 5492–5496.

Pearson, N.D., Eggleston, D.S., Haltiwanger, R.C., Hibbs, M., Laver, A.J., and Kaura, A.C. (2002) Design and synthesis of conformationally restricted eight-Membered ring diketones as potential serine protease inhibitors. *Bioorg Med Chem Lett* **12:** 2359–2362.

Pioletti, M., Schlunzen, F., Harms, J., Zarivach, R., Gluhmann, M., Avila, H., *et al.* (2001) Crystal structures of complexes of the small ribosomal subunit with tetracycline, edeine and IF3. *EMBO J* **20:** 1829–1839.

Porse, B.T., and Garrett, R.A. (1999) Sites of interaction of streptogramin A and B antibiotics in the peptidyl transferase loop of 23S rRNA and the synergism of their inhibitory mechanisms. *J Mol Biol* **286:** 375–387.

Poulsen, S.M., Karlsson, M., Johansson, L.B., and Vester, B. (2001) The pleuromutilin drugs tiamulin and valnemulin bind to the RNA at the peptidyl transferase centre on the ribosome. *Mol Microbiol* **41:** 1091–1099.

Pringle, M., Poehlsgaard, J., Vester, B., and Long, K.S. (2004) Mutations in ribosomal protein L3 and 23S ribosomal RNA at the peptidyl transferase center are associated with reduced susceptibility to tiamulin in Brachyspira spp. isolates. *Mol Microbiol* doi:10.1111/j.1365-2958.2004.04373.x

Schlunzen, F., Zarivach, R., Harms, J., Bashan, A., Tocilj, A., Albrecht, R., *et al.* (2001) Structural basis for the interaction of antibiotics with the peptidyl transferase centre in eubacteria. *Nature* **413:** 814–821.

Schlunzen, F., Harms, J.M., Franceschi, F., Hansen, H.A., Bartels, H., Zarivach, R., and Yonath, A. (2003) Structural basis for the antibiotic activity of ketolides and azalides. *Structure (Camb)* **11:** 329–338.

Schmeing, T.M., Seila, A.C., Hansen, J.L., Freeborn, B., Soukup, J.K., Scaringe, S.A., *et al.* (2002) A pre-translocational intermediate in protein synthesis observed in crystals of enzymatically active 50S subunits. *Nat Struct Biol* **9:** 225–230.

Sigmund, C.D., Ettayebi, M., and Morgan, E.A. (1984) Antibiotic resistance mutations in 16S and 23S ribosomal RNA genes of Escherichia coli. *Nucleic Acids Res* **12:** 4653–4663.

Springer, D.M., Sorenson, M.E., Huang, S., Connolly, T.P., Bronson, J.J., Matson, J.A., *et al.* (2003) Synthesis and activity of a C-8 keto pleuromutilin derivative. *Bioorg Med Chem Lett* **13:** 1751–1753.

Wallace, A.C., Laskowski, R.A., and Thornton, J.M. (1995) Ligplot – a program to generate schematic diagrams of protein ligand interactions. *Protein Engineering* **8:** 127–134.